Journal of
Water & Climate Change

IWA PUBLISHING

Journal of Water and Climate Change Vol 14 No 9, 3150 doi: 10.2166/wcc.2023.188

Application of hydrological models in climate change framework for a river basin in India

Rishith Kumar Vogeti [a], K. Srinivasa Raju [a,*], D. Nagesh Kumar [b], Advani Manish Rajesh [a], S. V. Somanath Kumar [a] and Yashraj Santosh Kumar Jha [a]

[a] Department of Civil Engineering, BITS Pilani, Hyderabad Campus, Hyderabad, India
[b] Department of Civil Engineering, Indian Institute of Science, Bangalore, India
*Corresponding author. E-mail: ksraju@hyderabad.bits-pilani.ac.in

RKV, 0000-0001-7493-4285

ABSTRACT

Soil Water Assessment Tool (SWAT), Hydrologic Engineering Center-Hydrologic Modelling System (HEC-HMS), and Hydrologic Simulation Program Fortran (HSPF) are explored for streamflow simulation of Lower Godavari Basin, India. The simulating ability of models is evaluated using four indicators. SWAT has shown exceptional simulating ability in calibration and validation compared to the other two. Accordingly, SWAT is used in the climate change framework using an ensemble of 13 Global Climate Models and four Shared Socioeconomic Pathways (SSPs). Three time segments, near-future (2021–2046), mid-future (2047–2072), and far-future (2073–2099), are considered for analysis. Four SSPs show a substantial increase in streamflow compared to the historical period (1982–2020). These deviations range from 17.14 (in SSP245) to 28.35% (in SSP126) (near-future), 31.32 (SSP370) to 43.28% (SSP585) (mid-future), and 30.41 (SSP126) to 70.8% (SSP585) (far-future). Across all timescales covering 948 months, the highest projected streamflows observed in SSP126, SSP245, SSP370, and SSP585 were 4962.36, 6,108, 6,821, and 6,845 m^3/s, respectively. Efforts are also made to appraise the influence of multi-model combinations on streamflow. The present study is expected to provide a platform for holistic decision-making, which helps develop efficient basin planning and management alternatives.

Key words: global climate models, HEC-HMS, HSPF, Lower Godavari Basin, streamflow, SWAT

HIGHLIGHTS

- SWAT performed ahead of HEC-HMS and HSPF in training and testing for all chosen indicators.
- Four SSPs show a substantial increase in streamflow compared to the historical period (1982–2020).
- Across all timescales, the highest projected streamflows observed in SSP126, SSP245, SSP370, and SSP585 were 4962.36, 6,108, 6,821, and 6,845 m^3/s, respectively.
- Four multi-model combinations were developed.

GRAPHICAL ABSTRACT

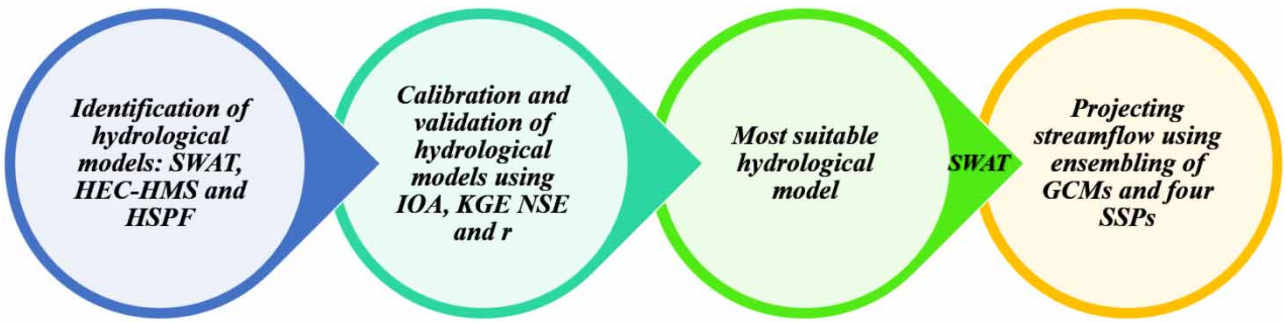

1. INTRODUCTION

Water, the lifeline of society, has a remarkable role in serving the needs of irrigation, industry, drinking, and others. Over time, these demands are increasing due to population growth, rapid urbanization, and industrialization (Heidari *et al.* 2021). Complementarily, the influence of climate change (CC) is evident as observed in the hydrological dynamics of the basin, mainly temperature and rainfall patterns (Jain & Singh 2020). These inadvertently affect the availability of water. In this context, it is essential to estimate the streamflow in a CC perspective for a river basin in a structured way. This assessment helps to formulate long-term basin planning and management measures (Okiria *et al.* 2022). Against this backdrop, process (Clark *et al.* 2017), conceptual (Reddy *et al.* 2023), lumped (Ghimire *et al.* 2020), physical (Al-Areeq *et al.* 2021), semi-distributed (Reddy & Pramada 2022), fully distributed (Bhanja *et al.* 2023), stochastic (Shabestanipour *et al.* 2023), deep learning (Sit *et al.* 2022), and hybrid deep learning (Ahmadi *et al.* 2023) based models were studied for the streamflow assessment by various researchers. Keeping this in view, choosing an appropriate model that accounts for high variability is always challenging. Another dimension is data availability, such as the climate and topography of the basin, soil type, land use, and streamflow. In this regard, the present investigation is an effort to study the suitability of three physically based hydrological models – the Soil Water Assessment Tool (SWAT), the Hydrologic Engineering Center-Hydrologic Modelling System (HEC-HMS), and the Hydrologic Simulation Program Fortran (HSPF) for streamflow simulation in the Lower Godavari Basin, India. These models were chosen due to their ease of use, limited data requirements, and suitability to diverse catchments (Beven 2019; Keller *et al.* 2022). A brief but related literature review is as follows:

Tan *et al.* (2019) simulated streamflows in Southeast Asia using SWAT, and the model demonstrated satisfactory performance as evidenced by the chosen metrics. They emphasized adapting the model to changing climatic, geographical, and land use conditions to improve its effectiveness. In continuation, numerous studies have employed the SWAT to review the effects of DEM (Goyal *et al.* 2018), LULC changes (Astuti *et al.* 2019), cumulative effects of DEM and LULC (Fan *et al.* 2021), resolution of soil and LULC (Kmoch *et al.* 2022), different precipitation scenarios (Zhang & Wang 2022), pre-processing methods on rainfall (Abbas & Xuan 2020), and calibration methods (Makumbura *et al.* 2022) on the performance. The earlier studies show that LULC has demonstrated a relatively higher impact on the model performance than other factors. Thus, it is essential to ensure the quality of LULC for deriving reliable streamflow predictions. Additionally, parameterization (White *et al.* 2017) is a crucial factor affecting the model performance. There is a scope for analysing the model by altering parameter combinations. However, SWAT performs exceptionally well when adequate spatio-temporal data is available.

HEC-HMS could be handy in streamflow simulation because its flexible model structure accommodates different loss, transform, routing, and baseflow methods. It requires relatively less pre-processing time and data compared to SWAT. Land use change due to urbanization significantly impacts the model performance (Ranjan & Singh 2022). Exploring several plausible HEC-HMS combinations may assist in identifying a suitable one that would yield promising estimates (Sahu *et al.* 2023).

Lampert & Wu (2018) explained in detail about HSPF, improvements, and challenges from the programming perspective. They also discussed the fusing of HSPF and high-level programming that handles most of the challenges. Wang *et al.* (2015) employed HSPF to study the effect of DEM resolution and rainfall on non-point source pollution (NPSP) and watershed hydrology modelling of the Yixunhe watershed, China. The effects of both could lead to uncertainty in streamflow estimation and NPSP. Similar studies are reported by Yan *et al.* (2014) in Jiaoyi Watershed, China, and Lee *et al.* (2023) in low-impact development practices.

Kazezyılmaz-Alhan *et al.* (2021) applied HEC-HMS and the rational method using the watershed management system for simulating event-based flood modelling across the Ayamama watershed, Turkey. It was concluded that HEC-HMS would be a viable tool for flood development plans in the basin compared to the lumped rational method.

Kumar & Bhattacharjya (2020) deployed SWAT and HEC-HMS to simulate the Alkhnanda and Bhagirathi rivers of Uttarakhand, India. SWAT performed slightly ahead of HEC-HMS based on NSE, RMSE, RMSE-standard ratio (RSR), and percent BIAS (PBIAS). Shekar & Vinay (2021) applied SWAT and HEC-HMS to simulate daily streamflow over the Hemavathi catchment, India. Based on R^2 and NSE, they found that SWAT has demonstrated better performance than HEC-HMS. Ferreira *et al.* (2021) used SWAT and HEC-HMS for simulating daily streamflow in Rio Grande Basin, Brazil. Based on NSE, PBAIS, and RSR, the SWAT has dominated HEC-HMS. Sempewo *et al.* (2023) employed HEC-HMS and SWAT for the event and continuous-based runoff simulation in Uganda's Manafwa and Sezibwa catchments. HEC-HMS was found suitable over SWAT based on *p*-scores obtained from the *t*-test.

Aqnouy *et al.* (2023) examined the streamflow behaviour of Oued Laou Watershed, Morocco, using ATelier Hydrologique Spatialisé (ATHYS), SWAT, and HEC-HMS. The SWAT is suitable compared to the other two based on R^2, NSE, PBIAS, and RSR. Further, it was also suggested that integrating models could be handy in reliable assessments.

Fenicia *et al.* (2007) opined that combining the outcomes of individual models using appropriate ensemble mechanisms would help boost the performance. Thus, it creates a scope for exploring various ensemble combinations to test their efficacy in different catchments. Some researchers also explored CC impact, which is as follows:

Kumar & Bhattacharjya (2020) compared SWAT and HEC-HMS for the Bhagirathi-Alkhnanda catchment, India. The SWAT was better than the others in the lean period. The impact of CC on future discharge was also studied for two Representative Concentration Pathways (RCPs). It was observed that the range of increase of peak discharge of Alkhnanda was 27–47% for two RCPs. Larbi *et al.* (2021) applied SWAT for the Vea catchment, West Africa, to evaluate the impact of CC on various aspects. They considered the RCP 4.5 scenario. An increase in mean annual temperature, evapotranspiration (ET), was identified, and contrarily, a decrease in surface runoff was observed. Ebodé *et al.* (2022) employed SWAT to estimate near-future and distant-future flows in the CC framework for Cameroon's So'o River Basin. They considered RCP 4.5 and 8.5. They also discussed temperature and precipitation fluctuations and corresponding streamflow changes. Guo *et al.* (2022) investigated the role of 21 Global Climate Models (GCMs) from Coupled Model Intercomparison Project Phase 6 (CMIP6) under three SSPs and 18 GCMs from CMIP5 framework under three RCPs to study runoff across the Yellow River Basin, China. Streamflow estimation from SWAT was found to increase for both CMIP6 and CMIP5. Ougahi *et al.* (2022) employed SWAT to visualize the influence of LULC on the Kabul River Basin using five GCMs and two RCPs. Water yield and ET were predicted to decrease. Phy *et al.* (2022) studied the impacts on the flow in the lower Prek Thnot River Basin, Cambodia. Three GCMs and two RCPs were considered. They integrated the Rainfall-Runoff-Inundation model and the SWAT. Flood magnitude, water level, and inundated areas were projected to vary compared to baseline scenarios. Ukumo *et al.* (2022) assessed the water availability in the Woybo catchment, Ethiopia using HEC-HMS. Multiple climate models and two RCPs were employed to project streamflow for 2050 and 2080. Rainfall and temperature were predicted to increase. An increase in discharge in 2050 and a decrease in 2080 were predicted. Tibangayuka *et al.* (2022) evaluated the influence on streamflow in the Upper Ruvu River watershed using HEC-HMS for 2041–2060 and 2081–2100. Climate studies were based on six GCMs and two RCPs. Streamflows were projected to increase in the two periods. Furthermore, limited studies were made on ensembling CMIP6 GCMs for various case studies (Mishra *et al.* 2020), whereas the advantages of ensembling GCMs were also discussed by Ngoma *et al.* (2021). Based on the literature review presented here and elsewhere, no studies were reported on

- applying HEC-HMS, SWAT, and HSPF simultaneously in the CMIP6 perspective and
- ensembling of GCMs and combining multi-model outputs simultaneously.

Accordingly, the objectives formulated are applied to LGB, India, which are as follows:

1. To study the suitability of SWAT, HEC-HMS, and HSPF.
2. To project streamflow using a suitable model (based on objective 1) from a CC perspective using an ensemble of CMIP6 GCMs with four SSPs.
3. To study the impact of combining the outputs of chosen hydrological models on streamflow.

Strengths of the present study include analysing streamflow for a major river basin in India using three hydrological and four resulting multi-model combinations. In addition, considering the impact of CC using a recently developed CMIP6 framework is an added advantage. Future streamflow in three time segments immensely helps officials develop strategies for sustainable water security.

Sections 2–7 describe the case study, methods, data collection, results, discussion, and conclusions.

2. CASE STUDY

Lower Godavari Basin (LGB) extends from 17°00′ to 19°00′N and 80°00′ to 83°4′E and borders Maharashtra, Andhra Pradesh, Odisha, Chhattisgarh, and Telangana. Its length and catchment area are 462 km and 39,180 km^2 (Figure 1). The basin experiences a tropical monsoon climate comprising two climatic regions, humid and dry sub-humid. The relative humidity is high in the basin during the southwest monsoon season, where maximum rainfall occurs. The highest relative

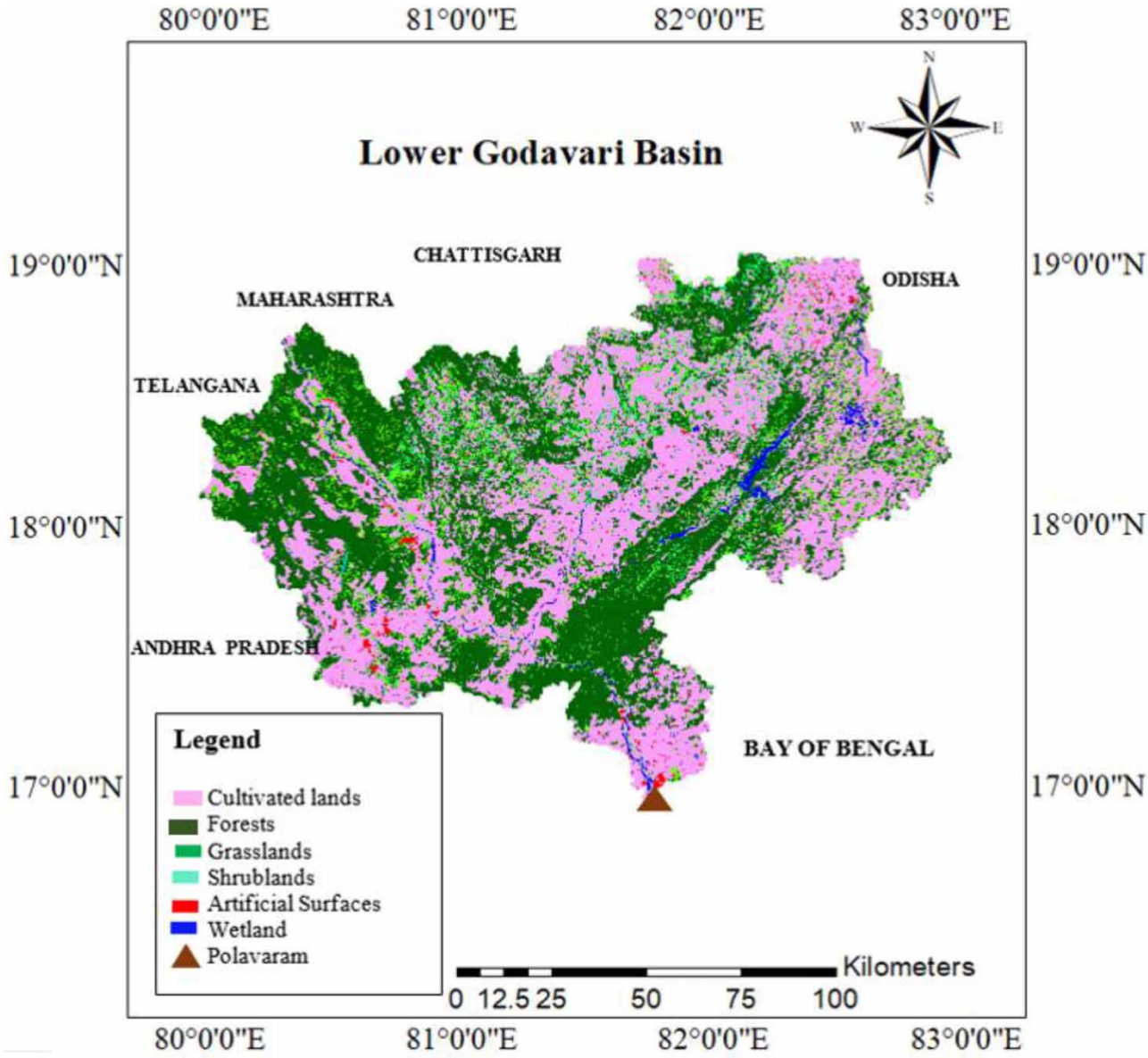

Figure 1 | Lower Godavari Basin in India.

humidity is observed from July to August and the lowest from April to May. Maximum relative humidity ranges from 60 to 89%, whereas minimum relative humidity varies from 15 to 29.5%.

The basin receives 1,096.92 mm annually (Sarkar 2022). The mean temperature varies from 26 to 44 °C. Annual evaporation values range from 1,401 to 2,606.40 mm (Jhajharia *et al.* 2021). Forests, cultivated land, artificial surfaces, grassland, wetland, and shrublands are the primary land covers in the basin. The soil conditions in the basin are diverse due to variations in geology and landforms. The most common soil types are red soil (alfisols) and black soil (vertisols). Loam and clayey loam black soils dominate this region. Requirements for drinking, agriculture, industry, canal stabilization, and inter-state dependencies necessitate quantifying streamflows for the basin (Polavaram Project Authority 2021).

3. DESCRIPTION OF METHODS

SWAT, HEC-HMS, HSPF, and statistical indicators used in this study are discussed here, including modules, parameters, and calibration processes. Water balance is the guiding principle for selecting the hydrological models.

SWAT used in the QGIS interface was QSWAT (Arnold *et al.* 2012). It facilitates various parameter combinations related to management, groundwater, soil, hydrologic response unit (HRU), soil, channel type, sub-basin, and basin. The following are the processes involved in modelling and the modules available in SWAT:

- *The watershed delineation module* facilitates the generation of the stream networks and delineation of the watershed by assigning an outlet.
- *HRUs module* enables importing the LULC, soil, and slope classes to generate HRU. This module also facilitates the reclassification of imported spatial databases.
- *Edit SWAT input database module* helps import the rainfall and temperature data, warm-up period, and time scale of calibration. It also creates tables to facilitate model runs.
- *The viewing output module* displays the global summary statistics of hydrological components. The simulated streamflow values can be saved in the output file.

The SWAT – Calibration and Uncertainty Procedure (SWAT-CUP) *interface* enables the calibration of parameters for streamflow simulation using four different algorithms. It can accommodate more than 400 parameters. Selected parameters with corresponding maximum and minimum values are presented in columns 2–4 of Supplementary Table S1 for an understanding of governing mechanism of SWAT. However, the results section discusses the basis of optimum values and related information.

HEC-HMS (Scharffenberg 2013) enables the computation of the streamflow of a basin. Relevant modules are:

- *Terrain data module* enables importing the DEM, pre-processing using GIS component to build stream network, and delineating the watershed.
- *The Basin module* enables the selection of loss, transform, baseflow, and routing methods. Methods that can be exercised in each component are mentioned as follows:
  - Loss methods (SCS-CN, initial and constant, initial and deficit, Green and Ampt, Soil Moisture Accounting, and Smith Parlange).
  - Transform processes (SCS-UH, Clark UH, ModClark, Kinematic wave transform, and Snyder UH).
  - Routing methods (Normal Depth, Modified Puls, Muskingum, Muskingum-Cunge).
  - Baseflow methods (Constant Monthly, Bounded Recession, Nonlinear Boussinesq and Recession, Linear Reservoir).
- *Meteorological and time series modules* enable importing of climate data into the model.
- *The control specifications module* accommodates space for several input records.
- *The optimization module* allows tuning the parameters using a univariate optimization technique.
- *The simulation module* helps calculate the streamflow and displays the statistics and graphs, which helps to interpret the model performance.

Selected parameters and related information are presented in Supplementary Table S2.

HSPF enables the estimation of the streamflow of a basin with relevant modules (Johanson *et al.* 1980). Relevant information is as follows:

- Better Assessment Science Integrating Point and Non-point Sources (BASINS) generates stream networks and delineation.
- The SARA time series utility function provides the meteorological data.
- The User Control File (UCI) enables the creation of three primary segments:
  - Pervious land (PERLND) from which water related to the pervious (PWATER) module can be obtained.
  - Impervious land (IMPLND) from which water related to the impervious (IWATER) module can be obtained. It consists of parameters associated with IWAT-PARM1, 2, 3, and IWAT-STATE1 sub-modules.
  - Reach or reservoir (RCHRES) from which water related to the reach and reservoir (HYDR) module can be obtained.
- The output tab enables streamflow simulation and interpretation of the performance.

Selected parameters and related information is presented in Supplementary Table S3.

Statistical indicators, Index of Agreement (IoA), Nash–Sutcliffe Efficiency (NSE) (Nash & Sutcliffe 1970), Kling Gupta Efficiency (KGE), and correlation coefficient (r) are chosen to assess the simulating ability of the hydrological models. KGE is based on the Eucledian distance philosophy covering correlation, bias, and variability (Gupta *et al.* 2009). IoA can detect the additional and proportional differences between means and variances (Willmott 1981). r specifies the strength of the

relationship between two continuous variables. Related mathematical expressions are as follows:

$$\text{IoA} = 1 - \frac{\sum_{i=1}^{n} (O_i - S_i)^2}{\sum_{i=1}^{n} (|S_i - \bar{O}| - |O_i - \bar{O}|)^2} \tag{1}$$

$$\text{NSE} = 1 - \frac{\sum_{i=1}^{n} (O_i - S_i)^2}{\sum_{i=1}^{n} (O_i - \bar{O})^2} \tag{2}$$

$$\text{KGE} = 1 - \sqrt{(r-1)^2 + \left(\frac{\sigma_{\text{Sim}}}{\sigma_{\text{Obs}}} - 1\right)^2 + \left(\frac{\bar{S}}{\bar{O}} - 1\right)^2} \tag{3}$$

$$r = \frac{\sum_{i=1}^{n} (O_i - \bar{O})\,(S_i - \bar{S})}{\sqrt{\sum_{i=1}^{n} (O_i - \bar{O})^2} \sqrt{\sum_{i=1}^{n} (S_i - \bar{S})^2}} \tag{4}$$

where O_i, S_i are the observed and simulated discharge (m^3/s); $\bar{O}$, $\bar{S}$ are the corresponding means whereas σ_{Obs}, σ_{Sim} are standard deviations, and n is the sample size.

SSP scenarios are used in CMIP6 to explore different futures of human society and their CC implications. Here, SSP126, SSP245, SSP370, and SSP585 refer to the first, second, third, and fifth trajectories reaching a radiative forcing of 2.6, 4.5, 7.0, and 8.5 W/m^2 by 2100. Narratives of the SSPs are as follows:

- SSP 126 visualizes a society focusing on sustainable development, low consumption, low population growth, reduced inequality, high economic growth, and low challenges for mitigation and adaptation.
- SSP245 emphasizes free markets, high consumption, moderate population growth, reduced inequality, moderate economic growth, and moderate challenges for mitigation and adaptation.
- SSP 370 focusses on security, high consumption, high inequality, socioeconomic growth, and high challenges for mitigation and adaptation.
- SSP585 focusses on free markets, high consumption, reduced inequality, high economic growth, high challenges for mitigation, and low for adaptation.

More details on SSPs are available in van Vuuren *et al.* (2017).

Relevant details of data required for modelling are presented in the next section.

4. DATA COLLECTION

The essential meteorological and spatial datasets for modelling are as follows:

- Rainfall and temperatures for 52 grid locations with a spatial grid resolution of 0.25° and 1°, respectively, for 1982–2020 were obtained from the India Meteorological Department. The temperature was further interpolated using the nearest neighbourhood interpolation method to achieve a resolution of 0.25°.
- Streamflow values for the Polavaram outlet of the basin from 1982 to 2020 were obtained from the Central Water Commission.
- A DEM tile with 30 m resolution was downloaded from the Shuttle Radar Topography Mission. The terrains in most of the basins were 'level to strongly rolling' in nature.
- The LULC map was obtained from GlobeLand30 of 30 m spatial resolution. The major extent of the basin consisted of cultivated land at 43.71% and forests at 42.13%.
- The soil map with a spatial resolution of 1 km was acquired from the Food Agriculture Organization. The composition of soil included loam (51.78%), clayey loam (27.8%), and sandy clayey loam (17.05%).

5. RESULTS

5.1. Model performance of SWAT, HEC-HMS, and HSPF from a historical perspective

The SWAT parameters were optimized in the SWAT-CUP interface using the Sequential Uncertainty Fitting algorithm. Eight SWAT parameter combinations ranging from 6 to 20 were evaluated using indicators, IoA, KGE, NSE, and *r* to determine the best one. The selected parameters were adjusted using absolute relative and replaced operators with 1,500 iterations. Parameter combinations with indicators exceeding the behaviour threshold were only considered for the analysis. Accordingly, 18 parameter combinations (CN2, ALPHA_BF, GW_DELAY, GWQMN, REVAPMN, GW_REVAP, ESCO, EPCO, CANMX, SOL_AWC, SOL_K, SOL_Z, SOL_BD, CH_N2, CH_K2, CH_N1, CH_K1, and SURLAG) (presented in column 2 in Supplementary Table S1) were identified. This combination has a slight edge over the other combinations explored with IoA, KGE, NSE, *r* of 0.94, 0.8, 0.8, and 0.91, respectively. The optimum values of these 18 parameters and inferences are presented in columns 4–5 of Supplementary Table S1. The SWAT-CUP interface also aids in interpreting the local sensitivity of these parameters, allowing ranking. However, in the present study, all 18 identified parameters are assumed equally sensitive to streamflow. It has also shown consistency in validation with an IoA, KGE, NSE, and *r* of 0.94, 0.56, 0.75, and 0.89, respectively. Significant underestimations (overestimations) were observed in the years 1987, 1990, 1994, and 2013 (1986, 2005, and 2009), respectively, for the calibration period (Figure 2(a) and 2(b)). In the validation, no underestimation was observed, whereas overestimation was found in 2015 and 2017 (Figure 2(a) and 2(b)).

The HEC-HMS parameters were calibrated using a univariate optimization method. This study explored six combinations of Loss, Transform, Baseflow, and Routing methods to understand suitable combinations that yield better simulation. It was noticed that SCS-CN-SCS-UH-Recession-Muskingum combination comprising nine parameters (IA, *I*, CN, T_{LAG}, Q_{INIT}, RC, RP, *K*, and *X*) (refer to column 2 of Supplementary Table S2) was preferred to the six combinations. Corresponding IoA, KGE, NSE, and *r* values in calibration were 0.87, 0.71, 0.62, and 0.78, respectively, whereas 0.76, 0.54, 0.41, and 0.7 were in validation. Corresponding optimum values and inferences are in columns 4–5 of Supplementary Table S2. Interestingly, KGE and NSE values are less in validation compared to calibration. Substantial underestimations (overestimations) in 1982, 1983, 1984, 1987, 1990, 1992, 1995, and 2013 (2014, 2016, 2018, and 2020) were observed in the calibration period. Underestimations (overestimations) were observed in 1986, 2000, 2003, 2009, and 2010 (2015 and 2017) in the validation period (Figure 2(a) and 2(b)).

HSPF parameters were calibrated using a manual method. A combination of IWAT-PARM2 and IWAT-STATE1 was found suitable (with relevant parameters LSUR, SLSUR, NSUR, RETSC, RETS, and SURS) among the four selected with an IoA, KGE, NSE, and *r* of 0.87, 0.73, 0.56, and 0.81, respectively. The corresponding optimum values and inferences are in columns 4–5 of Supplementary Table S3. A similar underestimation (overestimation) trend is observed for HSPF compared to other models (Figure 2(a) and 2(b)).

It is observed that SWAT showed exceptional performance over the HSPF and HEC-HMS (Figure 2(a) and 2(b)). Thus, the SWAT was further used in projecting streamflow in the LGB for 2021–2099 in four SSPs. The time horizon was split into three segments, namely, near-future (NF) (2021–2046), mid-future (MF) (2047–2072), and far-future (FF) (2073–2099). In addition, the impact of combining the outputs of chosen hydrological models, i.e., HEC + SWAT, SWAT + HSPF, HEC + HSPF, and HEC + SWAT-HSPF on streamflow was also studied and presented in the later section.

5.2. Projecting streamflow for 2021–2099

Rainfall and temperature predictions for 2021–2099 were collected from the repository of 13 GCMs for SSP126, SSP245, SSP370, and SSP585 (Mishra *et al.* 2020). It was observed that streamflows (from the suitable model, SWAT) increased in three time segments for all four SSPs compared to the baseline scenario (1982–2020). Efforts were also made to identify significant events (SEs) based on a threshold of 1,280 m^3/s. This value is nothing but the minimum of all Q_3 values.

Salient results are described in the following order: mean, percentage deviation of streamflow about the baseline, Q_1, Q_3, and the number of SE for each SSP (Nuzzo 2016).

- SSP126: NF are 1,175.73 m^3/s, 28.35, 982.7 m^3/s, 1,398 m^3/s, and 117. Changes in these values for MF (relative to NF) are 76.19 m^3/s, 6.2, 60.8 m^3/s, 43.25 m^3/s, and 19; 18.89 m^3/s, 2.05, −866.55 m^3/s, 1,096.68 m^3/s, and −8 for FF (relative to NF) (Figures 3(a) and 4(a)–4(c)).

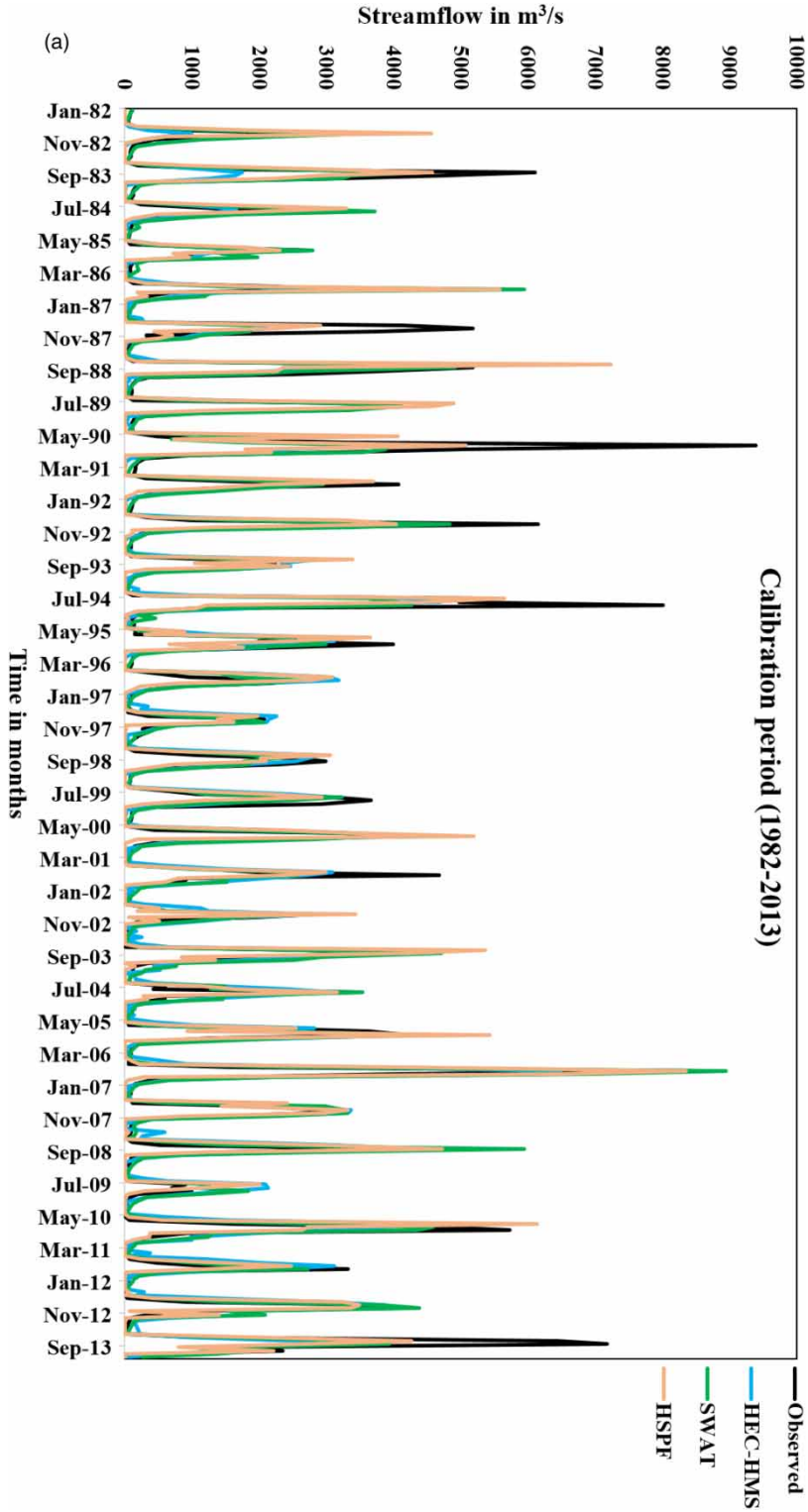

Figure 2 | Discharge plots for models in (a) calibration and (b) validation periods. (*continued.*).

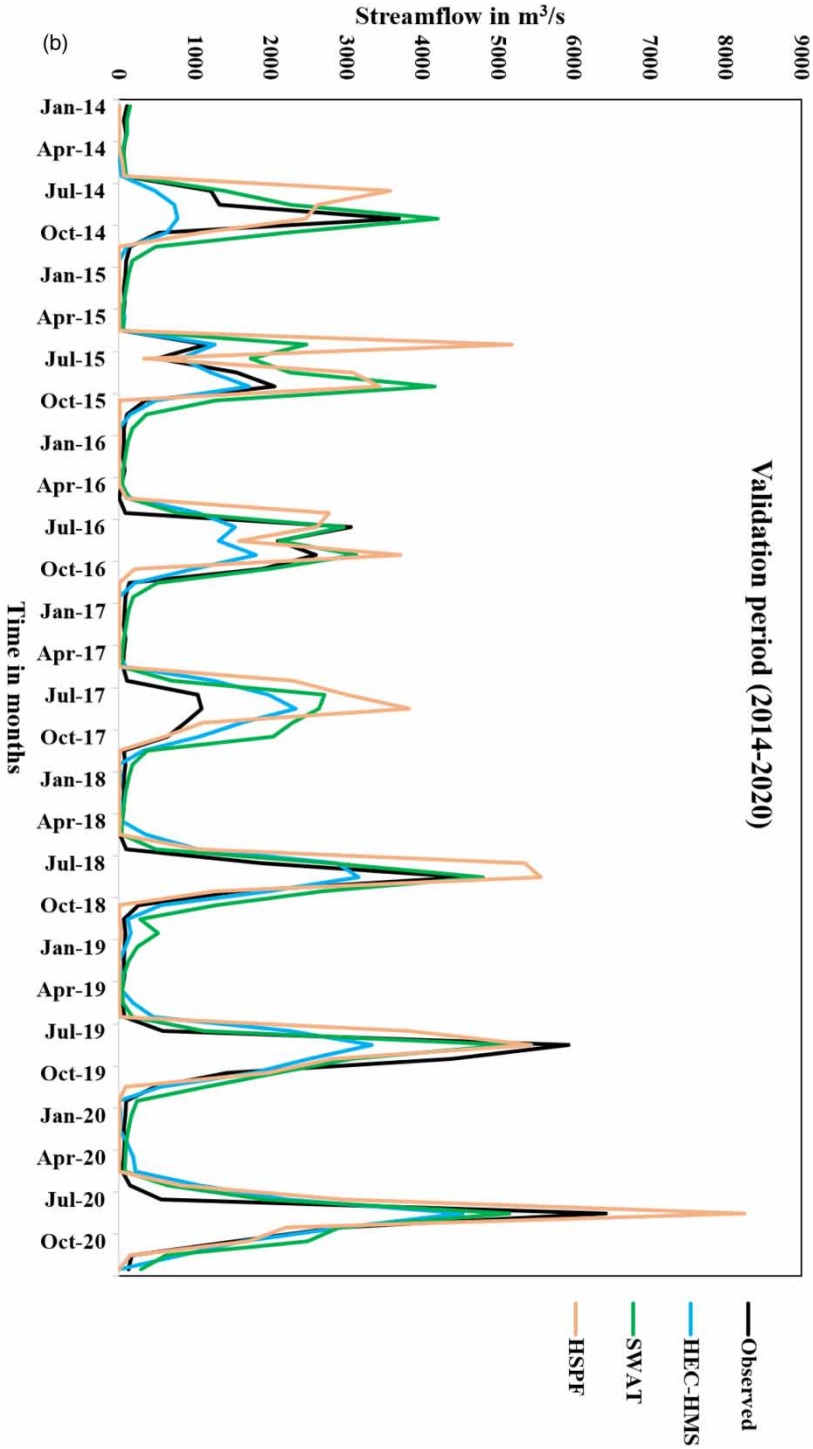

Figure 2 | Continued.

- SSP245: NF are 1,073.04 m^3/s, 17.14, 890.05 m^3/s, 1,280.5 m^3/s, and 78. Corresponding values in MF and FF relative to NF are increasing (except Q_1 in FF). Interestingly, the mean values and SE difference are relatively high (Figures 3(b) and 4(a)–4(c)).
- SSP370: NF are 1,115.61 m^3/s, 21.79, 939.13 m^3/s, 1,345.75 m^3/s, and 97. Similar inferences were that of SSP245 (Figures 3(c) and 4(a)–4(c)).

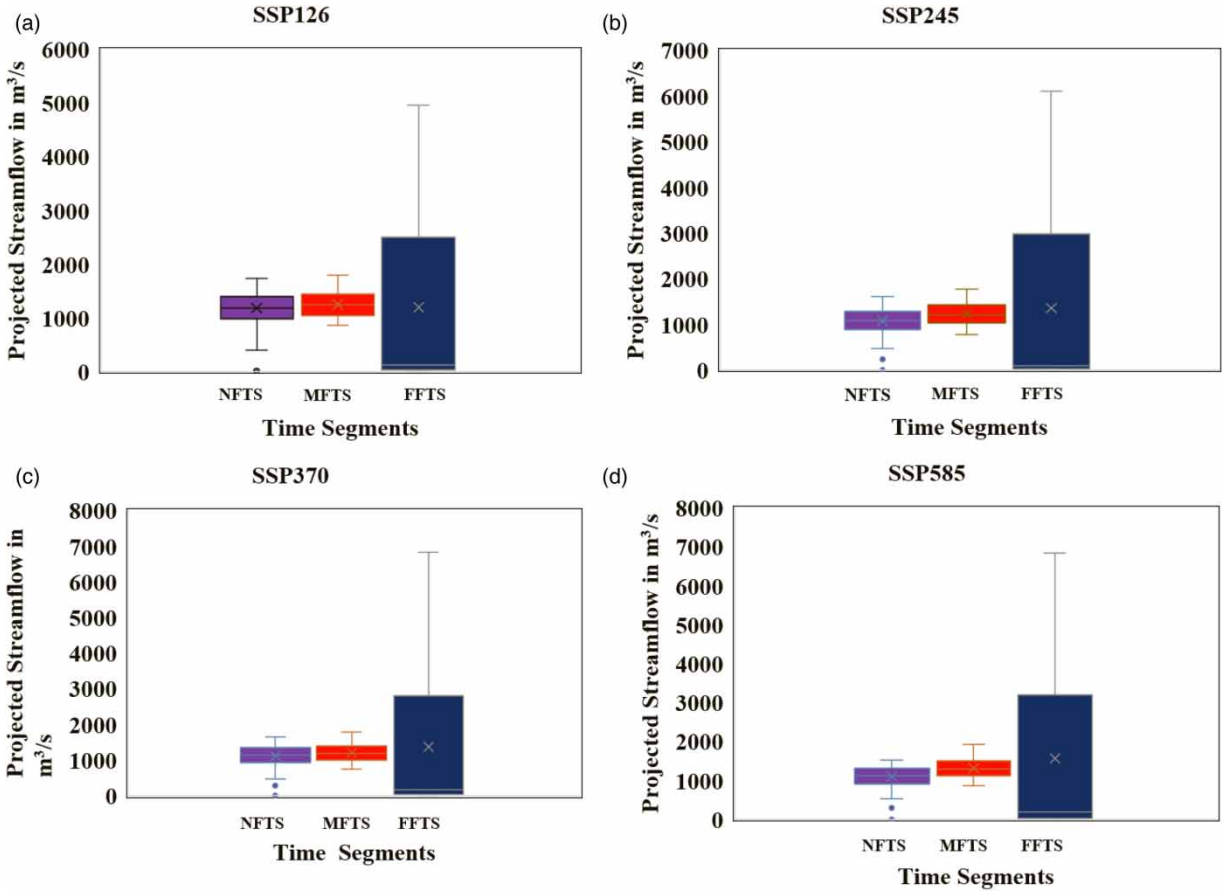

Figure 3 | Box and whisker plots for NF, MF, and FF using SWAT (a) SSP126, (b) SSP245, (c) SSP370, and (d) SSP585.

- SSP585: NF are 1,094.5 m^3/s, 19.48, 916.03 m^3/s, 1,302.5 m^3/s, and 88. Similar inferences were that of SSP245 (Figures 3(d) and 4(a)–4(c)).

Mean streamflow, deviation from baseline, Q_1, Q_3, and SE from SSP126 to SSP585 across *different time segments* show neither an upward nor downward trend. Related results are as follows:

- In NF, the order (highest to lowest) of parameters is SSP126, SSP370, SSP585, and SSP245.
- In MF, the order (highest to lowest) of parameters is SSP585, SSP126, SSP245, and SSP370, except for deviation from the baseline scenario. In this case, SSP585, SSP245, SSP126, and SSP370.
- In FF, the highest and lowest values tend to be observed in SSP585 and SSP370, respectively, for mean Q_3 and SE. Also, the highest deviation from the baseline can be observed in SSP370, followed by SSP585.
- The number of SE is relatively more in the MF scenario than in NF and FF. The highest number is 161 across all time scales for SSP585.
- The highest projected mean streamflow is 1,564.65 m^3/s, observed in the FF time segment under SSP585.

In summary, the range of deviation in projected streamflow observed across all four SSPs, 17.14–28.35% (NF), 31.32–43.28% (MF), and 30.41–70.8% (FF), indicate increment. Overall, it can be inferred that NF and MF exhibit low interquartile ranges compared to FF in all four SSPs. Predictions in FF challenge the policymakers due to low streamflow magnitudes in the lower quartile. Similar challenges in NF and FF, due to high values, sometimes double the upper quartiles discharge.

5.3. Effect of combining streamflows of hydrological models

Equal weighted averaging is employed to connect outputs of HEC and SWAT; SWAT and HSPF; HEC and HSPF; HEC, SWAT, and HSPF; to assess the impact of possible multi-models on streamflow. These combinations are termed *A*, *B*, *C*,

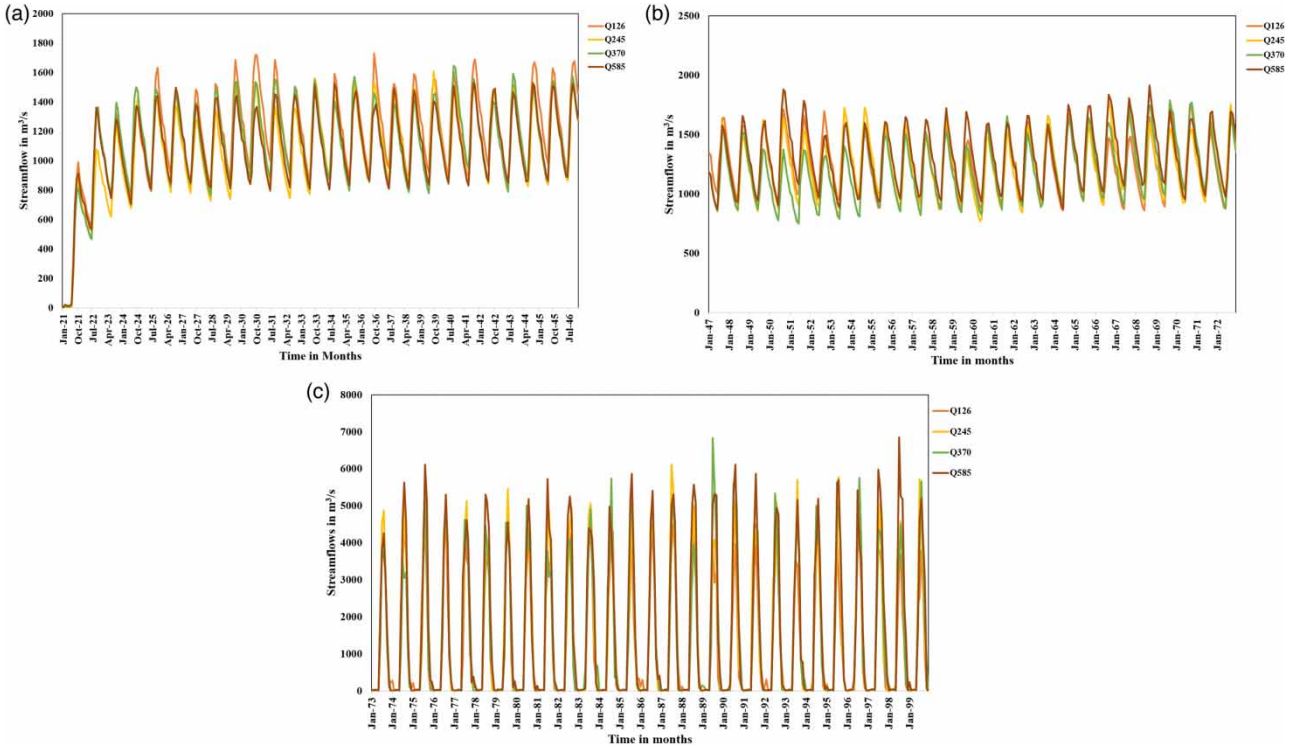

Figure 4 | (a–c) Projected streamflow in NF, MF, and FF time segments in four SSPs (Q126, Q245, Q370, and Q585-projected streamflow for SSP126, SSP245, SSP370, and SSP585, respectively).

and *D* for simple representation. Related results (mean streamflow and number of SE) of these combinations are compared with SWAT (suitable individual model) across SSPs and three time segments (Table 1). *Salient observations in comparison to SWAT are:*

- In SSP126, mean streamflow is more in the FF time segment and less in NF and MF for *A*. It is more in all time segments for B.
- It increased in MF and FF and decreased in NF for C and D. The three time segments' highest and lowest mean values are 1,329.42 and 1,034.93 m^3/s (occurred in *A*, respectively, for FF and NF). Higher and lower SE are 137 and 91, respectively.
- In SSP245, mean streamflow decreases in all time segments in *A* and *D*. The number of SE increased in NF and FF, whereas it is vice versa in MF for *A*, *B*, *C*, and *D*.
- In SSP370, the mean decreased in NF and FF, increasing in MF for *A*. It is declining in all time segments in *B* and *D*. SE decreased in NF and MF, whereas FF increased for A. There were patterns for *B*, C, and *D*.
- In SSP585, the mean decreased in all time segments in A, B, C, and D. SE increased in NF and FF in *A*, *B*, *C*, and *D*. It is vice versa for MF.

From a CC perspective, the highest streamflow observed is 1,564.65 m^3/s (Table 1). This may necessitate policymakers to analyse possible storage facilities required. It may lead to severe flooding if the situation is not suitably handled.

6. DISCUSSION

Calibration is an essential aspect affecting the streamflow simulation. The present study considers vast training data of 32 years, nearly three times the previous studies (Anshuman *et al.* 2018; Sharma & Regonda 2021). More training data enables the model to train for diverse climatic situations of the basin. According to Kunnath-Poovakka & Eldho (2019), simpler models represent fewer parameters and are ineffective at capturing spatially distributed flows influenced by land use, topography, and soil changes. Anshuman *et al.* (2018) and Reddy *et al.* (2023) drew similar inferences for long-term predictions.

Table 1 | Comparative analysis of SWAT and multi-model combination

SSP and time segment		SWAT		HEC-HMS + SWAT (A)		SWAT + HSPF (B)		HEC-HMS + HSPF (C)		HEC-HMS + SWAT + HSPF (D)							
		M (m^3/s)	*N*	*M* (m^3/s)	*N*	*M* (m^3/s)	*N*	*M* (m^3/s)	*N*	*M* (m^3/s)	*N*	Highest *M*	Lowest *M*	Difference in *M*	Highest *N*	Lowest *N*	Difference in *N*
SSP126	NF	1175.73	117	1034.93	91	**1239.28**	106	1098.48	104	1123.11	104	1239.28	1034.93	204.35	117	91	26
	MF	1251.92	136	1223.13	112	**1291.72**	115	1262.93	123	1258	119	1291.72	1223.13	68.59	136	112	24
	FF	1194.62	109	**1329.42**	137	1219.38	120	1304.66	125	1283.2	130	1329.42	1194.62	134.8	137	109	28
SSP245	NF	1073.04	78	984.21	89	**1125.81**	95	1036.98	97	1047.95	97	1125.81	984.21	141.6	97	78	19
	MF	1232.51	128	1227.81	112	**1238.46**	108	1233.76	116	1232.11	113	1238.46	1227.81	10.65	128	108	20
	FF	**1358.96**	114	1283.09	126	1312.92	122	1329.14	125	1307.07	127	1358.96	1283.09	75.87	127	114	13
SSP370	NF	**1115.61**	97	1022	93	1048.95	88	955.34	90	1007.75	90	1115.61	955.34	160.27	97	88	9
	MF	1202.97	114	**1203.15**	106	1091.84	87	1092.02	104	1127.87	102	1203.15	1091.84	111.31	114	87	27
	FF	1368.23	111	1363.26	134	1358.83	117	**1372.66**	122	1363.55	126	1372.66	1358.83	13.83	134	111	23
SSP585	NF	**1094.5**	88	1002.76	96	1034.56	91	942.82	97	992.39	97	1094.5	942.82	151.68	97	88	9
	MF	**1312.54**	161	1293.97	118	1308.26	112	1289.69	118	1296.01	114	1312.54	1289.69	22.85	161	112	49
	FF	**1564.65**	127	1487.8	148	1529.09	135	1523.36	134	1511.9	136	1564.65	1487.8	76.85	148	127	21
Highest		1564.65	161	1487.8	148	1529.09	135	1523.36	134	1511.9	136						
Lowest		1073.04	78	984.21	89	1034.56	87	942.82	90	992.39	90						
Difference		491.61	83	503.59	59	494.53	48	580.54	44	519.51	46						

Bold represents the highest value in each time segment across SSPs.

M indicates mean streamflow in m^3/s; *N* indicates the number of SE for a threshold of 1,280 m^3/s.

Further climate conditions of the basin also influence the suitability of the model. The present study is situated in humid and dry sub-humid conditions. It is humid subtropical, borderline Mediterranean, and oceanic type of climate for the study of Kazezyılmaz-Alhan *et al.* (2021), Tropical climate (Sempewo *et al.* 2023), Subtropical climate (Kumar & Bhattacharjya 2020), Humid subtropical (Shekar & Vinay 2021), and Sub-humid (Aqnouy *et al.* 2023). It is observed that SWAT was mostly found superior and suitable in different climate conditions.

According to the present study, the SWAT identified 18 parameters compared to 10 in HEC-HMS and 6 in HSPF. The improved performance of SWAT can be attributed to its ability to accommodate more parameters while accounting for the basin's spatial variability. CN2, SOL_AWC, ALPHA_BF, GW_REVAP, and ESCO were the most sensitive parameters similar to the studies reported by Saraf & Regulwar (2018) and Anshuman *et al.* (2018). These are SOL_AWC, CN2, and ESCO, as studied by Shekar & Vinay (2021), and SOL_AWC, ESCO, GW_DELAY, ALPHA_BF, CN2, and GWQMN suggested by Ferreira *et al.* (2021).

The SCS-CN-SCS-UH-Muskingum is the most suitable combination amongst HEC-HMS loss-transform-routing combinations for the present study and matches the analysis of Kumar & Bhattacharjya (2020). It is Green-Ampt-ClarkUH-Kinematic wave in the study of Kazezyılmaz-Alhan *et al.* (2021) and SMA-ClarkUH-Muskingum in the study of Sempewo *et al.* (2023).

The present study has witnessed slight underestimations in a few training and testing periods similar to that reported by Sharma & Regonda (2021). It requires a superior calibration mechanism, which can be considered for further study. The study is based on the climate variables corresponding to 13 CMIP6 GCMs (Mishra *et al.* 2020) that were bias-corrected, reducing systematic errors and consequently influencing the structural and scenario uncertainties (Wang *et al.* 2020).

Increasing streamflow trends were observed, echoing our studies for the far-future situation for SSP585; however, the difference in magnitude exists. No significant trend is observed for near- and mid-futures (Chatterjee *et al.* 2023; Mohseni *et al.* 2023; Reddy *et al.* 2023). Reddy *et al.* (2023) employed EC-Earth3, one of the 13 GCMs used. Mohseni *et al.* (2023) employed a simple average method over ACCESS-CM2, BCC-CSM2-MR, and CanESM5. Several studies reported high streamflows in the SSP585 (Reshma & ArunKumar 2023; Zhang *et al.* 2023).

The streamflows emanating from the four multi-model combinations deviate from those considered by Wan *et al.* (2021) and Gelete *et al.* (2023), due to various model combinations and averaging techniques. In general, results could significantly vary for different river basins due to climate changes, topography, land use, soil type, and other basin-related parameters., as evident from the studies of Fan *et al.* (2021), Kmoch *et al.* (2022), Zhang & Wang (2022), and Makumbura *et al.* (2022).

7. SUMMARY AND CONCLUSIONS

Streamflow projections are significant to policymakers for basin management. In this regard, SWAT, HEC-HMS, and HSPF were studied for their applicability, and their performance was evaluated using NSE, KGE, IOA, and *r*. SWAT performed ahead of the other two, and it was further used in projecting the streamflows in the near-future (2021–2046), mid-future (2047–2072), and far-future (2073–2099) time segments. The future climate variables over 13 CMIP6 GCMs were considered using a simple average. Four SSPs show a substantial increase in streamflow compared to the historical period. Across all timescales, the highest projected streamflows ascend from SSP126 to SSP585. Efforts are also made to examine the influence of multi-model combinations on streamflow and found to perform similarly to SWAT.

The present study is based on three hydrological models and 13 GCMs. Enough opportunity exists to include more appropriate models for a broader streamflow prediction. The study also can be extended with different ensembling mechanisms, indicators, and suitable SSP. SUFI-2 is considered in the present study for calibration, and enough scope exists to employ Ensemble Kalman Filter (EnKF) (Bayat *et al.* 2023).

ACKNOWLEDGEMENTS

This research work is sponsored by CSIR, New Delhi, through Project No. 22(0782)/19/EMR-II dated 24.7.19. The authors thank the officials for their support.

DATA AVAILABILITY STATEMENT

Data cannot be made publicly available; readers should contact the corresponding author for details.

CONFLICT OF INTEREST

The authors declare there is no conflict.

REFERENCES

Abbas, S. A. & Xuan, Y. 2020 Impact of precipitation pre-processing methods on hydrological model performance using high-resolution gridded dataset. *Water* **12** (3), 840.

Ahmadi, F., Tohidi, M. & Sadrianzade, M. 2023 Streamflow prediction using a hybrid methodology based on variational mode decomposition (VMD) and machine learning approaches. *Appl. Water Sci.* **13** (6), 135.

Al-Areeq, A. M., Al-Zahrani, M. A. & Sharif, H. O. 2021 The performance of physically based and conceptual hydrologic models: a case study for Makkah watershed, Saudi Arabia. *Water* **13** (8), 1098.

Anshuman, A., Eldho, T. I. & Poovakka, A. K. 2018 Performance evaluation of SWAT with a conceptual rainfall runoff model GR4J for a catchment in Upper Godavari River Basin. In: *Int. Soil Water Assess. Tool Conf.*, Vol. 101.

Aqnouy, M., Ahmed, M., Ayele, G. T., Bouizrou, I., Bouadila, A. & Stitou El Messari, J. E. 2023 Comparison of hydrological platforms in assessing rainfall-runoff behavior in a Mediterranean watershed of Northern Morocco. *Water* **15** (3), 447.

Arnold, J. G., Moriasi, D. N., Gassman, P. W., Abbaspour, K. C., White, M. J., Srinivasan, R. & Jha, M. K. 2012 SWAT: model use, calibration, and validation. *Trans. ASABE* **55** (4), 1491–1508.

Astuti, I. S., Sahoo, K., Milewski, A. & Mishra, D. R. 2019 Impact of land use land cover (LULC) change on surface runoff in an increasingly urbanized tropical watershed. *Water Resour. Manage.* **33**, 4087–4103.

Bayat, M., Alizadeh, H. & Mojaradi, B. 2023 Assimilation versus optimization for SWAT calibration: accuracy, uncertainty, and computational burden analysis. *Water Supply* **23** (3), 1189–1207.

Beven, K. 2019 How to make advances in hydrological modelling. *Hydrol. Res.* **50** (6), 1481–1494.

Bhanja, S. N., Coon, E. T., Lu, D. & Painter, S. L. 2023 Evaluation of distributed process-based hydrologic model performance using only a priori information to define model inputs. *J. Hydrol.* **618**, 129176.

Chatterjee, D., Singh, D., Singh, P. K., Fohrer, N. & Singh, B. B. 2023 Performance evaluation of different gridded precipitation and CMIP6 model products with gauge observations for assessing rainfall variability under the historical and future climate change scenario over a semi-arid catchment, India. *Phys. Chem. Earth Parts A/B/C* **131**, 103433.

Clark, M. P., Bierkens, M. F., Samaniego, L., Woods, R. A., Uijlenhoet, R., Bennett, K. E. & Peters-Lidard, C. D. 2017 The evolution of process-based hydrologic models: historical challenges and the collective quest for physical realism. *Hydrol. Earth Syst. Sci.* **21** (7), 3427–3440.

Ebodé, V. B., Dzana, J. G., Nkiaka, E., Nnomo, B. N., Braun, J. J. & Riotte, J. 2022 Effects of climate and anthropogenic changes on current and future variability in flows in the So'o River Basin (south of Cameroon). *Hydrol. Res.* **53** (9), 1203–1220.

Fan, J., Galoie, M., Motamedi, A. & Huang, J. 2021 Assessment of land cover resolution impact on flood modeling uncertainty. *Hydrol. Res.* **52** (1), 78–90.

Fenicia, F., Solomatine, D. P., Savenije, H. H. G. & Matgen, P. 2007 Soft combination of local models in a multi-objective framework. *Hydrol. Earth Syst. Sci.* **11** (6), 1797–1809.

Ferreira, R. G., Dias, R. L. S., de Siqueira Castro, J., dos Santos, V. J., Calijuri, M. L. & da Silva, D. D. 2021 Performance of hydrological models in fluvial flow simulation. *Ecol. Inform.* **66**, 101453.

Gelete, G., Nourani, V., Gokcekus, H. & Gichamo, T. 2023 Ensemble physically based semi-distributed models for the rainfall-runoff process modeling in the data-scarce Katar catchment, Ethiopia. *J. Hydroinf.* **25** (2), 567–592.

Ghimire, U., Agarwal, A., Shrestha, N. K., Daggupati, P., Srinivasan, G. & Than, H. H. 2020 Applicability of lumped hydrological models in a data-constrained river basin of Asia. *J. Hydrol. Eng.* **25** (8), 05020018.

Goyal, M. K., Panchariya, V. K., Sharma, A. & Singh, V. 2018 Comparative assessment of SWAT model performance in two distinct catchments under various DEM scenarios of varying resolution, sources and resampling methods. *Water Resour. Manage.* **32**, 805–825.

Guo, Y., Yu, X., Xu, Y. P., Wang, G., Xie, J. & Gu, H. 2022 A comparative assessment of CMIP5 and CMIP6 in hydrological responses of the Yellow River Basin, China. *Hydrol. Res.* **53** (6), 867–891.

Gupta, H. V., Kling, H., Yilmaz, K. K. & Martinez, G. F. 2009 Decomposition of the mean squared error and NSE performance criteria: implications for improving hydrological modelling. *J. Hydrol.* **377** (1–2), 80–91.

Heidari, H., Arabi, M., Warziniack, T. & Sharvelle, S. 2021 Effects of urban development patterns on municipal water shortage. *Front. Water* **3**, 694817.

Jain, C. K. & Singh, S. 2020 Impact of climate change on the hydrological dynamics of River Ganga, India. *J. Water Clim. Change* **11** (1), 274–290.

Jhajharia, D., Gupta, S., Mirabbasi, R., Kumar, R. & Patle, G. T. 2021 Pan evaporative changes in transboundary Godavari River basin, India. *Theor. Appl. Climatol.* **145**, 1503–1520.

Johanson, R. C., Imhoff, J. C. & Davis, H. H. 1980 *Users Manual for Hydrological Simulation Program-Fortran (HSPF)*, Vol. 80, No. 15. Environmental Research Laboratory, Office of Research and Development, USEPA.

Kazezyılmaz-Alhan, C. M., Yalçın, İ., Javanshour, K., Aytekin, M. & Gülbaz, S. 2021 A hydrological model for Ayamama watershed in Istanbul, Turkey, using HEC-HMS. *Water Pract. Technol.* **16** (1), 154–161.

Keller, A. A., Garner, K., Rao, N., Knipping, E. & Thomas, J. 2022 Hydrological models for climate-based assessments at the watershed scale: a critical review of existing hydrologic and water quality models. *Sci. Total Environ.* **869**, 161209.
Kmoch, A., Moges, D. M., Sepehrar, M., Narasimhan, B. & Uuemaa, E. 2022 The effect of spatial input data quality on the performance of the SWAT model. *Water* **14** (13), 1988.
Kumar, D. & Bhattacharjya, R. K. 2020 Evaluating two GIS-based semi-distributed hydrological models in the Bhagirathi-Alkhnanda River catchment in India. *Water Policy* **22** (6), 991–1014.
Kunnath-Poovakka, A. & Eldho, T. I. 2019 A comparative study of conceptual rainfall-runoff models GR4J, AWBM, and Sacramento at catchments in the upper Godavari river basin, India. *J. Earth Syst. Sci.* **128**, 1–15.
Lampert, D. J. & Wu, M. 2018 Automated approach for construction of long-term, data-intensive watershed models. *J. Comput. Civ. Eng.* **32** (4), 06018001.
Larbi, I., Hountondji, F. C., Dotse, S. Q., Mama, D., Nyamekye, C., Adeyeri, O. E. & Asare, Y. M. 2021 Local climate change projections and impact on the surface hydrology in the Vea catchment, West Africa. *Hydrol. Res.* **52** (6), 1200–1215.
Lee, H., Kim, J., Jun, S. M., Hwang, S., Song, J. H. & Kang, M. S. 2023 Analysis of the effects of low impact development practices on hydrological components using HSPF. *J. Hydro-Environ. Res.* **46**, 72–85.
Makumbura, R. K., Gunathilake, M. B., Samarasinghe, J. T., Confesor, R., Muttil, N. & Rathnayake, U. 2022 Comparison of calibration approaches of the Soil and Water Assessment Tool (SWAT) model in a Tropical Watershed. *Hydrology* **9** (10), 183.
Mishra, V., Bhatia, U. & Tiwari, A. D. 2020 Bias-corrected climate projections for South Asia from coupled model intercomparison project-6. *Sci. Data* **7** (1), 338.
Mohseni, U., Agnihotri, P. G., Pande, C. B. & Durin, B. 2023 Understanding the climate change and land use impact on streamflow in the present and future under CMIP6 climate scenarios for the Parvara Mula Basin, India. *Water* **15** (9), 1753.
Nash, J. E. & Sutcliffe, J. V. 1970 River flow forecasting through conceptual model. Part 1 – a discussion of principles. *J. Hydrol.* **10**, 282–290.
Ngoma, H., Wen, W., Ayugi, B., Babaousmail, H., Karim, R. & Ongoma, V. 2021 Evaluation of precipitation simulations in CMIP6 models over Uganda. *Int. J. Clim.* **41** (9), 4743–4768.
Nuzzo, R. L. 2016 The box plots alternative for visualizing quantitative data. *Statistically Speaking* **8** (3), 268–272.
Okiria, E., Okazawa, H., Noda, K., Kobayashi, Y., Suzuki, S. & Yamazaki, Y. 2022 A comparative evaluation of lumped and semi-distributed conceptual hydrological models: does model complexity enhance hydrograph prediction? *Hydrology* **9** (5), 89.
Ougahi, J. H., Karim, S. & Mahmood, S. A. 2022 Application of the SWAT model to assess climate and land use/cover change impacts on water balance components of the Kabul River Basin, Afghanistan. *J. Water Clim. Change* **13** (11), 3977–3999.
Phy, S. R., Try, S., Sok, T., Ich, I., Chan, R. & Oeurng, C. 2022 Integration of hydrological and flood inundation models for assessing flood events in the Lower Prek Thnot River Basin under climate change. *J. Hydrol. Eng.* **27** (10), 05022012.
Polavaram Project Authority. 2021 *Annual Report 2020–21 Ministry of Jal Shakti, Department of Water Resources, River Development & Ganga Rejuvenation*. Government of India.
Ranjan, S. & Singh, V. 2022 HEC-HMS based rainfall-runoff model for Punpun river basin. *Water Pract. Technol.* **17** (5), 986–1001.
Reddy, B. S. N. & Pramada, S. K. 2022 A hybrid artificial intelligence and semi-distributed model for runoff prediction. *Water Supply* **22** (7), 6181–6194.
Reddy, N. M., Saravanan, S., Almohamad, H., Al Dughairi, A. A. & Abdo, H. G. 2023 Effects of climate change on streamflow in the Godavari basin simulated using a conceptual model including CMIP6 dataset. *Water* **15** (9), 1701.
Reshma, C. & Arunkumar, R. 2023 Assessment of impact of climate change on the streamflow of Idamalayar River Basin, Kerala. *J. Water Clim. Change* **14** (7), 2133–2149.
Sahu, M. K., Shwetha, H. R. & Dwarakish, G. S. 2023 State-of-the-art hydrological models and application of the HEC-HMS model: a review. *Model. Earth Syst. Environ.* **9**, 3029–3051.
Saraf, V. R. & Regulwar, D. G. 2018 Impact of climate change on runoff generation in the Upper Godavari River Basin, India. *J. Hazard. Toxic Radioact. Waste* **22** (4), 04018021.
Sarkar, S. 2022 Drought and flood dynamics of Godavari basin, India: a geospatial perspective. *Arab. J. Geosci.* **15** (8), 772.
Scharffenberg, W. A. 2013 *Hydrologic Modeling System HEC-HMS User's Manual*. US Army Corps of Engineers.
Sempewo, J. I., Twite, D., Nyenje, P. & Mugume, S. N. 2023 Comparison of SWAT and HEC-HMS model performance in simulating catchment runoff. *J. Appl. Water Eng. Res.*, 1–15.
Shabestanipour, G., Brodeur, Z., Farmer, W. H., Steinschneider, S., Vogel, R. M. & Lamontagne, J. R. 2023 Stochastic watershed model ensembles for long-range planning: verification and validation. *Water Resour. Res.* **59** (2), e2022WR032201.
Sharma, V. C. & Regonda, S. K. 2021 Multi-spatial resolution rainfall-runoff modelling – a case study of Sabari river basin, India. *Water* **13** (9), 1224.
Shekar, N. C. S. & Vinay, D. C. 2021 Performance of HEC-HMS and SWAT to simulate streamflow in the sub-humid tropical Hemavathi catchment. *J. Water Clim. Change* **12** (7), 3005–3017.
Sit, M., Demiray, B. Z. & Demir, I. 2022 *A Systematic Review of Deep Learning Applications in Streamflow Data Augmentation and Forecasting*.
Tan, M. L., Gassman, P. W., Srinivasan, R., Arnold, J. G. & Yang, X. 2019 A review of SWAT studies in Southeast Asia: applications, challenges and future directions. *Water* **11** (5), 914.
Tibangayuka, N., Mulungu, D. M. & Izdori, F. 2022 Assessing the potential impacts of climate change on streamflow in the data-scarce Upper Ruvu River watershed, Tanzania. *J. Water Clim. Change* **13** (9), 3496–3513.

Ukumo, T. Y., Edamo, M. L., Abdi, D. M. & Derebe, M. A. 2022 Evaluating water availability under changing climate scenarios in the Woybo catchment, Ethiopia. *J. Water Clim. Change* **13** (11), 4130–4149.

van Vuuren, D. P., Riahi, K., Calvin, K., Dellink, R., Emmerling, J., Fujimori, S. & O'Neill, B. 2017 The Shared Socio-economic Pathways: trajectories for human development and global environmental change. *Global Environ. Change* **42**, 148–152.

Wan, Y., Chen, J., Xu, C. Y., Xie, P., Qi, W., Li, D. & Zhang, S. 2021 Performance dependence of multi-model combination methods on hydrological model calibration strategy and ensemble size. *J. Hydrol.* **603**, 127065.

Wang, H., Wu, Z. & Hu, C. 2015 A comprehensive study of the effect of input data on hydrology and non-point source pollution modeling. *Water Resour. Manage.* **29**, 1505–1521.

Wang, H. M., Chen, J., Xu, C. Y., Zhang, J. & Chen, H. 2020 A framework to quantify the uncertainty contribution of GCMs over multiple sources in hydrological impacts of climate change. *Earths Future* **8** (8), e2020EF001602.

White, J., Stengel, V., Rendon, S. & Banta, J. 2017 The importance of parameterization when simulating the hydrologic response of vegetative land-cover change. *Hydrol. Earth Syst. Sci.* **21** (8), 3975–3989.

Willmott, C. J. 1981 On the validation of models. *Phys. Geogr.* **2**, 184–194.

Yan, C. A., Zhang, W. & Zhang, Z. 2014 Hydrological modeling of the Jiaoyi watershed (China) using HSPF model. *Sci. World J.* **2014**, 627360.

Zhang, J. & Wang, Y. 2022 Runoff prediction under different precipitation scenarios based on SWAT model and stochastic simulation of precipitation. *J. Hydrol. Eng.* **27** (5), 05022003.

Zhang, S., Gan, T. Y., Bush, A. B. & Zhang, G. 2023 Evaluation of the impact of climate change on the streamflow of major pan-Arctic river basins through machine learning models. *J. Hydrol.* **619**, 129295.

First received 20 March 2023; accepted in revised form 15 August 2023. Available online 28 August 2023